Applied Physics Letters

Electron and hole deep levels related to Sb-mediated Ge quantum dots embedded in n-type Si, studied by deep level transient spectroscopy

Victor-Tapio Rangel-Kuoppa, Alexander Tonkikh, Peter Werner, and Wolfgang Jantsch

Citation: Appl. Phys. Lett. **102**, 232106 (2013); doi: 10.1063/1.4809595
View online: http://dx.doi.org/10.1063/1.4809595
View Table of Contents: http://apl.aip.org/resource/1/APPLAB/v102/i23
Published by the AIP Publishing LLC.

Electron and hole deep levels related to Sb-mediated Ge quantum dots embedded in n-type Si, studied by deep level transient spectroscopy

Victor-Tapio Rangel-Kuoppa,[1,a)] Alexander Tonkikh,[2,b),c)] Peter Werner,[2,d)] and Wolfgang Jantsch[3,e)]
[1]*Institut de Ciència de Materials de Barcelona (ICMAB), Campus de la UAB, Bellaterra 08193, Barcelona, Spain*
[2]*Max Planck Institute of Microstructure Physics, Weinberg 2, D-06120, Halle (Saale), Germany*
[3]*Institute of Semiconductor- and Solid State Physics, Johannes Kepler Universität, A-4040 Linz, Austria*

(Received 23 January 2013; accepted 15 May 2013; published online 13 June 2013)

The deep level transient spectroscopy technique is used on a Ti Schottky diode on n-Si with embedded Ge quantum dots (QDs) obtained by Sb-mediated growth. We discover an electron trap and two hole traps within the Si band gap at the plane of the Ge QDs. The electron trap has an activation energy of 87 ± 7 meV. One hole trap has an activation energy of 304 ± 32 meV, The second hole trap is represented by an energy sub-band between 125 and 250 meV above the top of the Si valence band. The electron level (87 ± 7 meV) and the hole energy sub-band (125–250 meV) are identified as energy levels of the Ge QDs array. The deepest trap level for holes (304 meV) has not been identified yet. © *2013 AIP Publishing LLC*. [http://dx.doi.org/10.1063/1.4809595]

Ge quantum dots (QDs) have been a hot research topic in recent years. As they are easily incorporated into the well developed SiGe technology, they have been extensively studied, with respect to their quantum confinement properties. It is expected that these confinement properties will open the possibility of new technological and industrial applications. For example, QDs are expected to be used in various applications such as mid-infrared spectral photodetectors,[1] Si-compatible spin-based quantum information processing,[2] quantum information processing, due to entanglement of confined electrons, holes or excitons,[3] intermediate band solar cells,[4] for use in thermoelectric and energy saving applications, as they have proven to significantly reduce the thermal conductivity while keeping high electrical conductivity.[5,6] This vast spectrum of possibilities has triggered fundamental research on Ge QDs in a Si matrix.[7–15]

The formation mechanism known as Stranski-Krastanov growth mode is used to obtain Ge QDs in Si. According to this mechanism, after a few monolayers of two-dimensional growth, the Ge film transforms into an array of Ge islands. These islands are then capped with Si forming the array of Ge QDs in Si. The size and shape of the Ge QDs are strongly affected by the growth conditions.[16] In particular, the use of a surfactant (Sb) improves the shape uniformity and luminescence properties of Ge QDs grown by molecular beam epitaxy (MBE).[17,18] Due to their small size, these Sb-mediated Ge QDs may confine charge carriers in all three dimensions yielding quantum levels, which act as deep-level traps for holes and electrons.[12–14]

Two samples were grown on n-type Si(100) substrates having a resistivity of $5\,\Omega\cdot$cm. The first sample (S1) was grown in the following way. After thermally removing the SiO_2 from the substrate surface, a monolayer thick Sb ad-layer is deposited to the substrate surface. This layer is used during growth as a reservoir for background doping and to accommodate the δ-doping. Moreover, this Sb ad-layer mediates the formation of Ge QDs making them smaller and improving their size homogeneity.[17] Next step was the deposition of a 200 nm thick Si buffer layer at 520 °C. Sb segregation and incorporation in the buffer layer has led to a desired background doping of approximately 10^{17} cm^{-3}. This doping procedure was similar to that one used in Ref. 19. Then, a Sb-δ-doped layer was formed at a substrate temperature of 480 °C. The δ-Sb-doping is used to enhance the amount of electric charges trapped by Ge QDs. On top of this δ-layer, a 5 nm thick undoped Si layer is grown. Then, a Ge layer having a nominal thickness of 1.1 nm was deposited to form an array of Ge islands. These Ge islands were capped with a 10 nm thick undoped Si layer forming Ge QDs in Si. The undoped Si layers and Ge QDs were grown at 620 °C. The growth of this structure is finished with a 20 nm thick n-type Si layer deposited at 520 °C. The deposition rates of Ge and Si were 0.02 and 0.05 nm/s, respectively. At these growth conditions the array of Sb-mediated Ge QDs should have a density of about 1.5×10^{11} cm^{-2}.[18] The sequence for the second sample (S2) was similar to the one done for the sample S1 up to the δ-Sb-doped layer. On top of the δ-Sb-doped layer in the sample S2, a 5 nm thick Sb-doped n-type Si layer was deposited followed by the Ge QDs layer capped with a 15 nm thick n-type Si layer. The only QD layer is also grown at 620 °C in this sample. The sequence of as grown layers and doping details of the samples S1 and S2 are depicted in Fig. 1(a).

The presence of the Ge QDs in our samples was confirmed by cross-section dark-field TEM (CSDF-TEM), as in former studies.[17,18] (see Fig. 1(b)). At the same time, our TEM study reveal a dislocation density smaller than 4×10^6 cm^{-2}.[20]

An important parameter characterizing electron and hole traps is their activation energy (E_{act}), which is required to

a)Email: tapio.rangel@gmail.com
b)Also at the Institute for Physics of Microstructures RAS, GSP-105 Nizhniy Novgorod, Russia
c)Email: tonkikh@mpi-halle.de
d)Email: werner@mpi-halle.de
e)Email: wolfgang.jantsch@jku.at

take a charge carrier from the deep level to an energy band edge. As the Sb-mediated growth technique for Ge QDs has been introduced only recently, the electrical characteristics of these Ge QDs have not been established yet. Therefore, in this study, we applied the standard deep level transient spectroscopy (DLTS) technique as a proven technique to determine energy levels within Sb-mediated Ge QDs grown in n-type Si by MBE.[13,21–24] A DL-82E equipment from Semilab is used.

The samples S1 and S2 were prepared for electrical characterization in a similar way as in former studies.[13,14] Briefly, samples were first covered with 200 nm SiO_2 by plasma enhanced chemical vapor deposition. An alloyed AuSb ohmic contact was first formed on the back-side of the substrate. The alloying temperature was 360 °C for 5 min in N_2 atmosphere. Afterwards, using standard photolithographic techniques, such as those described in Ref. 25, a Ti Schottky contact with an area $A = 0.3\,\mathrm{mm}^2$ was deposited on the epilayer. The sample was glued to the sample holder with Fixogum, to ensure good thermal contact.[26]

C-V measurements were done at room temperature. Results are shown in Fig. 2(a). In the inset, the C^{-2} vs V analysis has revealed that the desired background doping concentration of the Si buffer layer was achieved in both samples.

The C-V measurements show that the desired background doping concentration of Si was achieved in both samples. Therefore, the built-in electric field of the Ti-Si Schottky diode reaches the Si buffer layer. The Ge QDs are thus situated inside the depleted region of the Ti-Si Schottky diode. Fig. 2(b) shows schematically the band diagram of the sample S2 at 300 K, when no external bias is applied. The gray area represents the depletion region, which is approximately 57 nm wide at a zero bias. Quantum wells for holes are formed in the Ge QDs, while for electrons the Ge QDs are barriers. However, a strain-induced conduction band bending in Si next to the QDs plane leads to potential wells for electrons at the QD interface,[27] which are depicted in Fig. 2(b) by two dips in the conduction band. It is important to note that this strain-induced conduction band bending dips happen in the Ge QDs plane as well, but for clarity purposes they are not depicted in Fig. 1(b).

The DLTS investigation was carried out at a constant frequency of $\omega = 1\,\mathrm{MHz}$ within the temperature range of 50–250 K. At the same time, the equivalent series resistance R_s was measured. The quality factor $Q = \omega\, C_S R_s$ was calculated, and it was found to always be $Q \ll 1$. Thus, measurements were not distorted by any large value of R_s.[23,28]

Several DLTS measurements were done on both samples, using seven different repetition rates of 2.5, 2.2, 2, 1.8, 1.6, 1.4, and 1.2 kHz. The DLTS scans were measured at a zero bias, and deep levels were populated using a forward bias pulse of +1 V and 5 μs duration. This procedure has the following advantages:

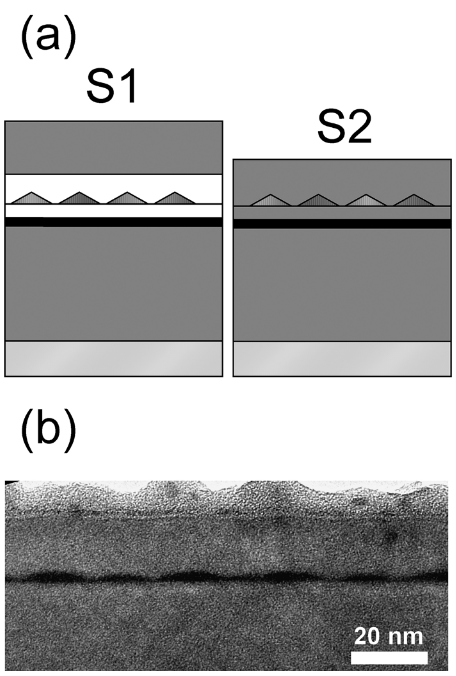

FIG. 1. (a) Cross-section scheme of samples S1 and S2; (b) cross-section TEM image of sample S2, dark clusters are Ge-rich regions referred to as Ge QDs.

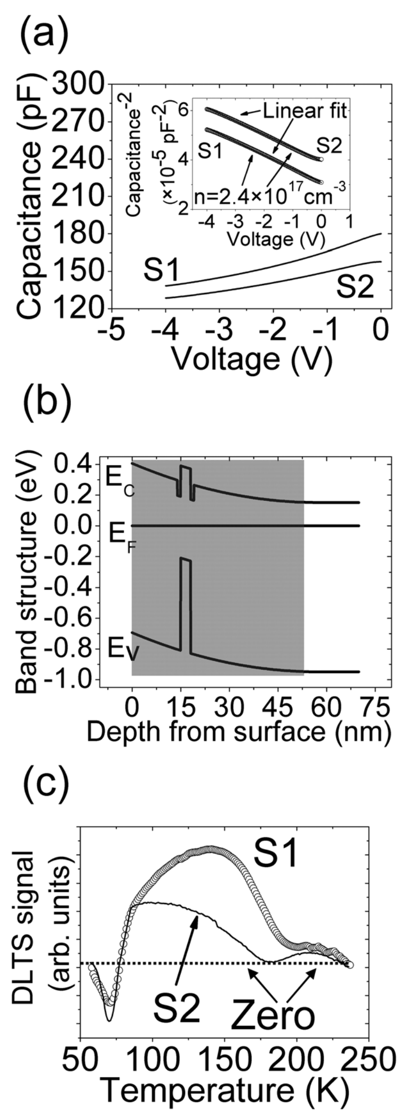

FIG. 2. (a) CV measurements done on samples S1 and S2. In the inset, the C^{-2} vs V analysis is shown, (b) schematic view of the band structure for sample S2, and (c) representative DLTS measurements for the samples S1 and S2. The repetition rates were 2.5 kHz, the pulse length was 5 μs. The zero of the DLTS signal is shown.

(i) DLTS scans are not affected by any leakage current.
(ii) The detection of both minority and majority carrier deep levels is possible, since both electrons and holes are injected with a forward bias.
(iii) No DLTS signal appears from the interface epilayer/substrate, since the depleted region does not reach this interface region between the epilayer and the substrate.[21,22,24]

Two representative DLTS plots, taken at a repetition rate of 2.5 kHz, are shown in Fig. 2(c).

As the measurement temperature increases, a first deep level signal can be seen for both samples at around 75 K. This signal is a downward peak, which corresponds to a majority carrier trap, and hence, it is an electron deep level.[21,22] Two additional DLTS signals are observed at higher temperatures. One signal is found between 80 and 180 K, and the other one—between 180 K and 250 K. Both are upward peaks, hence, minority carrier DLTS signals, i.e., DLTS signals of holes.[21,22] The DLTS signal of the electron level for sample S2 appears slightly stronger than in the sample S1, see Fig. 2. We assume that the cause for this effect is higher n-type doping at the Ge QDs layer in the sample S2 as compared to sample S1. The higher n-type doping allows more electrons to be trapped in QDs. Therefore, DLTS signals of hole traps are weaker in sample S2 than in sample S1. Since, more electrons are available in the vicinity of the Ge QDs layer in the sample S2, hole capture by Ge QDs is hindered.

The emission rate (e) of a deep level having the activation energy E_{act} is related to the absolute temperature (T) by

$$e \sim T^2 \exp\left(-\frac{E_{act}}{kT}\right), \qquad (1)$$

where k is the Boltzmann constant.[21,22] The value of e equals the repetition rate where the DLTS reaches a minimum or a maximum, and thus, e is related with the value of T at which the minimum or maximum in the DLTS spectra occurs.[21,22] In this way, the e vs T relation was obtained. Thus, the value of E_{act} for a deep-level trap could be extracted from the linear fitting of the Arrhenius plot of $\ln(\frac{e}{T^2})$. These plots are shown in Figs. 3(a) and 3(b) for the downward peak at 70 K and the upward peak at 220 K, respectively. The analysis of the DLTS signal between 80 K and 220 K was done by deconvoluting the signal, as shown in Fig. 3(c). Five DLTS signals with activation energies of 125, 159, 196, 231, and 300 meV, respectively, yield the peaks P1–P5 peaks in Fig. 3(c), respectively.

A value of $E_{act} \sim 88$ meV is found for the electron level, while for the hole DLTS signal around 220 K, a value of $E_{act} \sim 300$ meV is obtained. This value is used in the deconvolution process shown in Fig. 3(c), as peak P5.

Usually, DLTS provides activation energies with an accuracy of 5%–10%.[22] Hence, the values of E_{act} obtained via deconvolution, can be considered as a hole sub-band encompassing the peaks P1–P4, spanning an energy interval from 125 to 250 meV.

We assume that the broad energy spectrum of the hole sub-band is caused by the size dispersion of Ge QDs. This fact correlates with the results of our recent investigations of photo- and electroluminescence of Sb-mediated Ge QDs.[17,18] At the same time, our CSDF-TEM images reveal a concentration of dislocations, five orders of magnitude smaller than the Ge QD density. Thus, dislocations play a negligible role for the DLTS signal. The size dispersion of QDs is responsible for the broadening of their luminescence band, which has a full width at half maximum of about 120–130 meV at 300 K. The latter band width is very close to the value obtained by DLTS for the hole sub-band. Moreover, the band of photon energies (E_{ph}) emitted by these QDs is well fitted by the equation $E_{ph} = E_G^{Si} - E_{act}^e - E_{act}^h$, whereas the luminescence band width is given as a sum of electron and hole subbands obtained by DLTS: $\Delta E_{ph} = \Delta E_{act}^e + \Delta E_{act}^h$. The latter parameters are obtained from DLTS measurements and simulations. After the substitution of these parameters into the equation for E_{ph}, we obtain an energy band at 720–970 meV, which is well matched by the luminescence band of Sb-mediated Ge QDs.[17,18] Therefore, we identified the electron and the hole sub-band as the aggregate of energy states at the interface of Ge QDs and within Ge QDs, respectively. Schematically, the

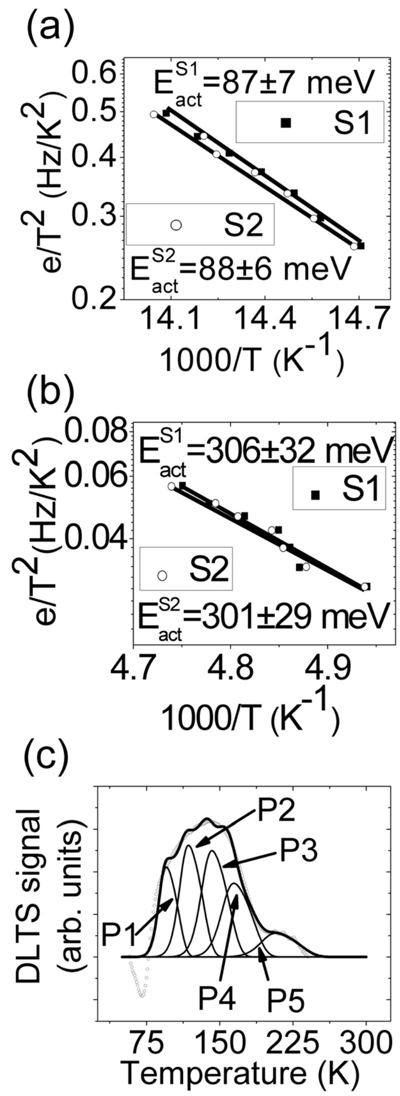

FIG. 3. Linear fit and Arrhenius plots for DLTS signals located at around (a) 75 K, (b) 220 K in samples S1 and S2, and (c) deconvolution process done on the DLTS signal done for sample S1 shown in Fig. 2, using five peaks P1, P2, P3, P4, and P5, with activation energies of 125, 159, 196, 231, and 300 meV.

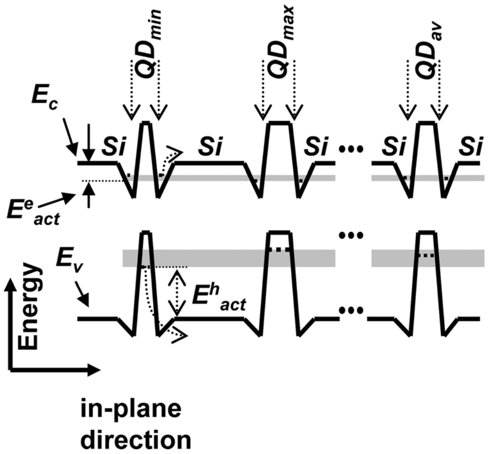

FIG. 4. Scheme of energy bands of the array of Sb-mediated Ge QDs in Si; E_v and E_c are valence and conduction band edges; QD_{min}, QD_{max}, and QD_{av} represent QDs of minimum, maximum, and mean sizes; E^e_{act} and E^h_{act} are electron and hole activation energies, shaded rectangles represent energy spans for electronic and hole sub-bands caused by QDs size dispersion.

band diagram for this situation is depicted in Fig. 4. The origin of the second deep level found at the plane of Ge QDs ($E_{act} \sim 300$ meV, P5 in Fig. 3(c)) is not clear yet. This level may be related to a specific defect within Sb-mediated QDs, which does not show up in luminescence experiments. The nature of this deep hole trap will be the subject of future investigations.

In summary, the results of a DLTS study on Sb-mediated Ge QDs embedded in n-type Si, grown by the Sb-mediated MBE method, have been reported. We found one electron level having an activation energy of 87 ± 7 meV and two hole level signals. One hole level is well fitted by an activation energy of 304 ± 32 meV. However, the other hole level signal cannot be explained by a single activation energy. We assume that the second signal is caused by the broad sub-band or by the convolution of several hole levels within energies spanning from 125 meV to 250 meV. The strongest signal in this hole sub-band comes from a hole level having an activation energy of 200 meV above the top of the Si valence band. The comparison of our present results with our recent luminescence studies on Sb-mediated Ge QDs leads us to the assumption that the electron level and the hole sub-band represent aggregate states within Ge QDs array, while the origin of the deepest hole trap remains unclear.

Victor-Tapio Rangel-Kuoppa gratefully acknowledges the National Council for Science and Technology (CONACyT) of México, postdoctoral fellowship 78965, the Fonds zur Förderung der Wissenschaftlichen Forschung (Vienna, Austria), the PLATON-SiN project of FFG (Vienna, Austria), project 20550, and Consejo Superior de Investigaciones Cientificas (CSIC) from Spain. Alexander Tonkikh gratefully acknowledges the support of the BMBF and DFG foundations.

The authors would like the thank Elisabeth Pachinger, Alma Halilovic, Ursula Kainz, Eckehard Nusko, Otmar Fuchs, Stephan Bräuer, and Andreas Frommfeld for expert technical assistance.

[1]A. I. Yakimov, A. I. Nikiforov, V. A. Timofeev, A. A. Bloshkin, V. V. Kirienko, and A. V. Dvurechenskii, Semicond. Sci. Technol. **26**, 085018 (2011), and Refs. 8–13 therein.
[2]S. Ketharanathan, S. Sinha, J. Shumway, and J. Drucker, J. Appl. Phys. **105**, 044312 (2009), and Refs. 1 and 2 therein.
[3]A. I. Yakimov, G. Y. Mikhalyov, A. V. Dvurechenskii, and A. I. Nikiforov, J. Appl. Phys. **102**, 093714 (2007), and Refs. 1 to 9 therein.
[4]A. M. Kechiantz, L. M. Kocharyan, and H. M. Kechiyants, Nanotechnology **18**, 405401 (2007).
[5]P. D. Lacharmoise, A. Bernardi, A. R. Goñi, M. I. Alonso, M. Garriga, N. D. Lanzillotti-Kimura, and A. Fainstein, Phys. Rev. B **76**, 155311 (2007).
[6]J. Alvarez-Quintana, X. Alvarez, J. Rodriguez-Viejo, D. Jou, P. D. Lacharmoise, A. Bernardi, A. R. Goñi, and M. I. Alonso, Appl. Phys. Lett. **93**, 013112 (2008), and Refs. 1 to 10 therein.
[7]A. Yakimov, A. V. Dvurechenskii, A. I. Nikiforov, A. A. Bloshkin, A. V. Nenashev, and V. A. Volodin, Phys. Rev. B **73**, 115333 (2006).
[8]A. Yakimov, A. V. Dvurechenskii, V. A. Volodin, M. D. Efremov, A. I. Nikiforov, and G. Y. Mikhalyov, Phys. Rev. B **72**, 115318 (2005).
[9]J. Drucker, IEEE J. Quantum Electron. **38**, 975 (2002).
[10]K. Brunner, Rep. Prog. Phys. **65**, 27 (2002).
[11]S. K. Zhang, H. J. Zhu, F. Lu, Z. M. Jiang, and X. Wang, Phys. Rev. Lett. **80**, 3340 (1998).
[12]M. Grydlik, M. Brehm, F. Hackl, H. Groiss, T. Fromherz, F. Schaeffler, and G. Bauer, New J. Phys. **12**, 063002 (2010).
[13]V.-T. Rangel-Kuoppa, A. Tonkikh, N. Zakharov, P. Werner, and W. Jantsch, Solid State Phenom. **178**, 67 (2011).
[14]V.-T. Rangel-Kuoppa, G. Chen, and W. Jantsch, Solid State Phenom. **178**, 72 (2011).
[15]M. Grydlik, G. Langer, T. Fromherz, F. Schaeffler, and M. Brehm, Nanotechnology **24**, 105601 (2013).
[16]V. G. Dubrovskii, G. E. Cirlin, Yu. G. Musikhin, Yu. B. Samsonenko, A. A. Tonkikh, N. K. Polyakov, V. A. Egorov, A. F. Tsatsul'nikov, N. A. Krizhanovskaya, V. M. Ustinov, and P. Werner, J. Cryst. Growth **267**(1–2), 47–59 (2004).
[17]A. Tonkikh, N. Zakharov, V. Talalaev, and P. Werner, Phys. Status Solidi (RRL) **4**, 224 (2010).
[18]A. A. Tonkikh, N. D. Zakharov, A. V. Novikov, K. E. Kudryavtsev, V. G. Talalaev, B. Fuhrmann, H. S. Leipner, and P. Werner, Thin Solid Films **520**, 3322–3325 (2012).
[19]D. V. Yurasov, M. N. Drozdov, A. V. Murel, M. V. Shaleev, N. D. Zakharov, and A. V. Novikov, J. Appl. Phys. **109**, 113533 (2011).
[20]See supplementary material at http://dx.doi.org/10.1063/1.4809595 for a plan-view image of the single Sb-mediated Ge quantum dot sample. The image field is about 25 μm^2. No dislocations are seen. This means, we have less than 4×10^6 dislocations/cm^2.
[21]D. V. Lang, J. Appl. Phys. **45**, 3023 (1974).
[22]V.-T. Rangel-Kuoppa, "Electrical characterization of nitrogen containing III-V semiconductors," Doctoral Thesis (Helsinki University of Technology, Helsinki, Finland, 2007).
[23]V.-T. Rangel-Kuoppa, A. Tukiainen, and J. Dekker, Microelectron. J. **34**, 751 (2003).
[24]V.-T. Rangel-Kuoppa, Appl. Phys. Lett. **100**, 252110 (2012).
[25]V.-T. Rangel-Kuoppa and A. Conde-Gallardo, Thin Solid Films **519**, 453 (2010).
[26]V.-T. Rangel-Kuoppa and G. Chen, Rev. Sci. Instrum. **81**, 036102 (2010).
[27]S.-V. Kondratenko, S.-L. Golovinskiy, O. V. Vakulenko, Y.-N. Kozyrev, M.-Y. Rubezhanska, and A.-I. Vodyanitsky, Surf. Sci. **601**, L45 (2007).
[28]V.-T. Rangel-Kuoppa and M. Pessa, Rev. Sci. Instrum. **74**, 4561 (2003).